Journal of Molecular Spectroscopy 379 (2021) 111496

Contents lists available at ScienceDirect

Journal of Molecular Spectroscopy

journal homepage: www.elsevier.com/locate/yjmsp

Article

Anion photoelectron spectroscopic and relativistic coupled-cluster studies of uranyl dichloride anion, $UO_2Cl_2^-$

Mary Marshall, Zhaoguo Zhu, Junzi Liu, Kit H. Bowen, Lan Cheng *

Department of Chemistry, The Johns Hopkins University, Baltimore, MD 21218, USA

ARTICLE INFO

Keywords:
Coupled-cluster
Anion photoelectron
Uranyl

ABSTRACT

A joint relativistic coupled-cluster and experimental photoelectron (PE) spectroscopic study of the uranyl dichloride anion, $UO_2Cl_2^-$, is reported. Sophisticated electronic-structure calculations predict the photodetachment of $UO_2Cl_2^-$ to involve a U 5f electron and to be followed by significant geometry relaxation. Therefore, the adiabatic electron affinity (EA_a) of the uranyl dichloride neutral molecule, UO_2Cl_2, and the vertical detachment energy (VDE) of its anion, $UO_2Cl_2^-$, provide valuable information about its uranium 5f orbital energies. The EA_a value was computed to be 3.15 eV. The VDE value was calculated to be 3.55 eV by augmenting the computed EA_a with a shift derived from a Franck–Condon simulation using coupled-cluster potential energy surfaces. The VDE, which corresponds to the highest intensity peak in the PE spectrum, was measured to be 3.69 ± 0.20 eV, in good agreement with the computed value. The origin transition in the PE spectrum, whose electron binding energy corresponds to the EA_a, was assigned to the feature at 3.2 ± 0.20 eV, consistent with the computed EA_a.

1. Introduction

The chemistry of the uranyl ion $[O–U–O]^{2+}$, an important building block in many uranium compounds, is among the central topics of actinide chemistry [1–4]. For example, uranyl-containing molecules play important roles in uranium separation science. In the plutonium uranium redox extraction (PUREX) process, a standard nuclear reprocessing method, uranium is extracted as uranyl nitrate coupled to the tributylphosphate extractant [5]. The uranyl ion comprises two strong uranium–oxygen bonds and forms relatively weak bonds with ligands in many important uranium species, e.g., the $UO_2Cl_4^{2-}$ formal dianion in the $Cs_2UO_2Cl_4$ crystal consists of a uranyl ion weakly coupled to four chlorines. Understanding the interactions between the uranyl ion with ligands thus is of fundamental importance.

Numerous experimental and theoretical efforts [6–60] have been devoted to study of the uranyl ion, resulting in a better understanding of many aspects of uranyl-containing molecules. Experimental studies of electronic and vibrational spectra of UO_2Cl_2, the target molecule of the present study, have been reported in non-aqueous solvents [8], in its crystal structure [10], and in noble gas matrices [15]. Based on the measured absorption and emission spectra, the structures of UO_2Cl_2 in solvents were found to be similar to those of crystalline uranyl salts. Heaven et al. studied UO_2Cl_2 in an argon matrix, which minimally perturbs the molecule. Through laser-induced fluorescence, the lowest energy transition observed in emission spectra occurred at 20323 cm^{-1} with nearly harmonic vibrational progressions at a frequency of 840 cm^{-1} [15]. This is similar to transitions seen in uranyl salts in the condensed phase and in solution [2,8]. The dominant vibrational progression is due to the U–O symmetric stretch. The O–U–O angle was found to be slightly bent, i.e., to be around 168 degree, in the normally linear UO_2^{2+}. Minor discrepancies between measured vibrational frequencies for the O–U–O symmetric bending mode and calculations of gas-phase molecules were attributed to van der Waals repulsion between the oxygen atoms and the argon matrix [15].

When a uranyl-containing anion differs from the corresponding neutral molecule by a uranium 5f electron, e.g., $UO_2Cl_2^-$ is formed by adding a 5f electron to UO_2Cl_2, the adiabatic electron affinity of the neutral molecule provides direct information about its uranium 5f orbital energies and thus is of fundamental interest. Wang and collaborators have reported the measurements of the electron affinities for uranium oxides UO_n, with n = 1-5 [23,61,62]. The adiabatic electron affinity value of UO_2 was accurately determined to be 1.1688(6) eV [62]. With two unpaired 5f electrons already present in UO_2, however, the electron affinity of UO_2 is expected to differ substantially from those of uranyl-containing molecules. On the other hand, because of the remarkable stability of the uranyl ion, UO_3, UO_4, and UO_5 can in general be considered as having a uranyl ion bonded with the other oxygen atoms. The variation of the measured electron affinity values of

* Corresponding author.
E-mail addresses: kbowen@jhu.edu (K.H. Bowen), lcheng24@jhu.edu (L. Cheng).

https://doi.org/10.1016/j.jms.2021.111496
Received 30 April 2021; Received in revised form 5 June 2021; Accepted 6 June 2021
Available online 11 June 2021

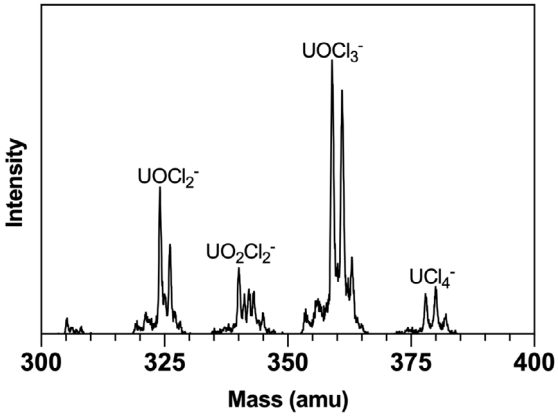

Fig. 1. The mass spectrum obtained from laser ablating a uranium rod in the presence of a 0.5% HCl and 0.5% O_2 in a He gas mixture. The $UO_2Cl_2^-$ anion mass peaks occur at 340, 342, and 344 amu.

1.12 eV, 3.60 eV, and 4.02 eV for UO_3, UO_4, and UO_5 [23] reflect the effects of the bonding with the additional oxygen atoms on the uranyl 5f orbital energies. Wang and collaborators have also reported photoelectron spectroscopic studies of uranyl tetrahalide dianions, $UO_2X_4^{2-}$ (X = F or Cl) [20], and uranyl trihalide anions, $UO_2X_3^-$ (X = F, Cl, Br, or I) [21]. These photoelectron spectra provided detachment energies for the corresponding uranyl-containing systems involving electrons in the U–O bonding orbital or from the ligands.

In this paper we report a joint experimental and computational study of the photoelectron spectrum of the uranyl dichloride anion, $UO_2Cl_2^-$, aiming to discern the adiabatic electron affinity (EA_a) for the uranyl dichloride molecule, UO_2Cl_2, and the vertical detachment energy (VDE) of its anion, $UO_2Cl_2^-$. Relativistic exact two-component coupled-cluster (CC) calculations were performed to predict the EA_a value of UO_2Cl_2 and the VDE value of $UO_2Cl_2^-$ to guide the analysis of its complex anion photoelectron spectrum. Details about the experimental and computational studies are presented in Sections 2 and 3. Computational results and the measured spectra are discussed in Section 4 to determine the VDE value of $UO_2Cl_2^-$ and the EA_a value of UO_2Cl_2. Finally, a summary and an outlook are provided in Section 5.

2. Experimental details

The experiments were conducted using a laser vaporization source with our anion photoelectron spectrometer, which has described previously [63]. Briefly, a depleted uranium rod was used as the laser vaporization target. A backing gas consisting of 0.5% HCl and 0.5% O_2 in He was simultaneously expanded over the surface of the rod. The resulting anions were extracted and analyzed using a time-of-flight mass spectrometer. Fig. 1 presents a mass spectrum showing the variety of anions that were produced by the source, comprising uranium, oxygen, and chlorine. Since the depleted uranium rod is essentially isotopically pure U-238, the isotopic pattern of chlorine assisted in assigning the anions to their corresponding mass peaks. The mass peaks at 340, 342, and 344 amu are $UO_2Cl_2^-$ and follow the predicted isotopic pattern of the anion. Two other anions ($UO_2Cl_2H^-$ and UCl_3^-) also contribute to the mass spectrum in the 340 to 350 amu range.

The photoelectron spectra (PES) of $UO_2Cl_2^-$ were obtained by photodetaching the 340 amu anion since it has the highest intensity. The $UO_2Cl_2^-$ anions were mass selected, decelerated, and crossed with a fixed frequency photon beam, 355 nm (3.49 eV) and 266 nm (4.66 eV) Nd:YAG laser. The resultant detached electrons were energy-analyzed using a magnetic bottle energy analyzer. The time of flight spectrum is converted to electron binding energy using the Levenberg–Marquardt algorithm and calibrated against the known transitions of Cu^- [64]. The photodetachment process is governed by the energy-conserving relationship, hv = EKE + EBE, where EKE is the electron kinetic energy and EBE is the electron binding energy. The resolution of the energy analyzer is about 50 meV at EKE = 1 eV. The photoelectron spectra presented are the average of multiple spectra.

3. Computational details

Given the roles of relativistic and spin–orbit effects in actinide-containing molecules and anions, calculations involving them are challenging and require high-level computational methods. In the present work, all relativistic coupled-cluster calculations were performed using the CFOUR [65–72] program package. Geometry optimizations for the ground state of UO_2Cl_2 and the four lowest scalar-relativistic states of $UO_2Cl_2^-$ were carried out at the coupled-cluster singles and doubles with noniterative triples [CCSD(T)] [73,74] level using correlation-consistent triple-zeta (cc-pVTZ) [75,76] basis sets. Scalar-relativistic effects were treated using the spin-free exact two-component theory in its one-electron variant (SFX2C-1e) [69,77,78] and cc basis sets contracted for the SFX2C-1e scheme (cc-pVXZ-X2C). The 6s, 6p, 7s, 5f electrons of U, 3s, 3p electrons of Cl, and 2s, 2p electrons of O were correlated in these calculations. SFX2C-1e equation-of-motion electron-attachment CCSD (EOMEA-CCSD) [79] calculations were also performed in the optimized structures of the anion to demonstrate the orbital composition of the unpaired electron.

The adiabatic electron affinity (EA_a) of $UO_2Cl_2^-$ was then calculated using optimized structures for the electronic ground state of UO_2Cl_2 and $UO_2Cl_2^-$. SFX2C-1e-CCSD(T) calculations using uncontracted cc-pVTZ and cc-pVQZ (cc-pVTZ-unc and cc-pVQZ-unc) basis sets were carried out and the electron-correlation energies were extrapolated using a two-parameter formula [80]

$$E_{\mathrm{corr}}[\infty \mathrm{Z}] = E_{\mathrm{corr}}[\text{cc-pVXZ}] - c/X^3, \quad (1)$$

to estimate the basis-set-limit values. Since this is a detachment of a uranium 5f electron, spin–orbit (SO) coupling makes significant contribution to the detachment energy. CCSD(T)/cc-pVTZ-unc calculations in combination with exact two-component Hamiltonian [81–83] with atomic mean-field [84] spin–orbit integrals (X2CAMF) [71] were performed to obtain EA_a with non-perturbative inclusion of spin–orbit coupling. The SO correction is then obtained as the difference between X2CAMF and SFX2C-1e CCSD(T)/cc-pVTZ-unc results. The U 5d, 6s, 6p, 7s, 5f electrons, Cl 3s and 3p electrons, and O 2s and 2p electrons were correlated in these energy calculations using uncontracted basis sets, while virtual orbitals with orbital energies higher than 100 Hartree were kept frozen in the CC step. The zero-point vibrational energy (ZPE) contribution to EA_a was obtained using harmonic frequencies of UO_2Cl_2 and UO_2Cl_2 obtained at SFX2C-1e-CCSD(T)/cc-pVTZ level by means of numerical differentiation of analytic gradients [68].

A Franck–Condon (FC) simulation of vibrational progression for the transition from the electronic ground state of $UO_2Cl_2^-$ to that of UO_2Cl_2 was performed within the harmonic approximation at the SFX2C-1e-CCSD(T)/cc-pVTZ level. The difference between the maximal peak position of the FC spectrum and the vibrational origin transition is added to EA_a to obtain the vertical detachment energy (VDE). The computation of the FC overlap used a highly efficient implementation in the fcsquared module [70] of the CFOUR program. The extra electron in the anion is located in a localized uranium 5f orbital, which can be well described by cc-pVTZ or cc-pVQZ basis sets. The effects of diffuse functions on the structures and energies thus are small, i.e., less than 0.005 Å for bond lengths, less than 1 degree for bond angles, and less than 0.005 eV for the adiabatic electron affinity. Therefore, we have used the cc-pVXZ, X = T, Q basis sets for uranium throughout our study.

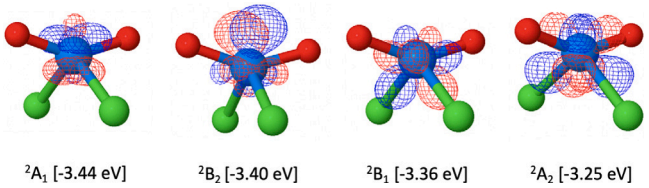

Fig. 2. Molecular orbitals in which the unpaired electrons in the lowest scalar-relativistic states of $UO_2Cl_2^-$ are located. The O, Cl, and U atoms are colored in red, green, and cyan, respectively. The vertical electronic energy difference with respect to the neutral molecule obtained from SFX2C-1e-EOMEA-CCSD/cc-pVTZ calculations are enclosed in the brackets.

Table 1
Structural parameters (bond lengths in Å and bond angles in degree) computed at the SFX2C-1e-CCSD(T)/cc-pVTZ level for UO_2Cl_2 and $UO_2Cl_2^-$.

		R[U–O]	R[U–Cl]	∠[O–U–O]	∠[Cl–U–Cl]
UO_2Cl_2	$^1A_1$	1.755	2.531	165.8	109.5
$UO_2Cl_2^-$	$^2A_1$	1.835	2.679	145.9	113.8
	$^2B_2$	1.835	2.687	145.8	114.3
	$^2B_1$	1.822	2.677	153.0	117.2
	$^2A_2$	1.816	2.692	159.3	121.9

Table 2
Harmonic vibrational frequencies (in cm^{-1}) computed at SFX2C-1e-CCSD(T)/cc-pVTZ level for the ground state of UO_2Cl_2 and the ground state of $UO_2Cl_2^-$.

	$UO_2Cl_2^-$	UO_2Cl_2
a_1 (sym. Cl–U–Cl bending)	57	56
b_1 (asym. O–U–O/Cl–U–Cl bending)	117	150
a_1 (sym. O–U–O bending)	121	206
a_2 (twisting)	193	177
b_2 (out-of-plane)	188	232
a_1 (sym. U–Cl stretching)	263	341
b_2 (asym. U–Cl stretching)	280	339
a_1 (sym. U–O stretching)	823	915
b_1 (asym. U–O stretching)	906	990

Table 3
The computed adiabatic electron affinity (EA_a) and vertical detachment energy (VDE) values (in eV) of UO_2Cl_2. The HF values for EA_a were obtained using the cc-pVQZ-unc basis sets. The correlation contributions were obtained using the cc-pVTZ-unc and cc-pVQZ-unc basis sets and extrapolated to estimate the basis-set-limit value.

	HF	CCSD	CCSD(T)	+SO[a]	+ZPV[b]
EA_a	3.087	2.961	2.820	3.125	3.153
VDE[c]	3.484	3.358	3.217	3.522	3.550

[a]Spin–orbit corrections (difference between X2CAMF and SFX2C-1e calculations).
[b]zero-point vibrational contribution.
[c]Obtained by augmenting computed EA_a with a shift of 0.397 eV derived from the Franck–Condon simulation in Fig. 3.

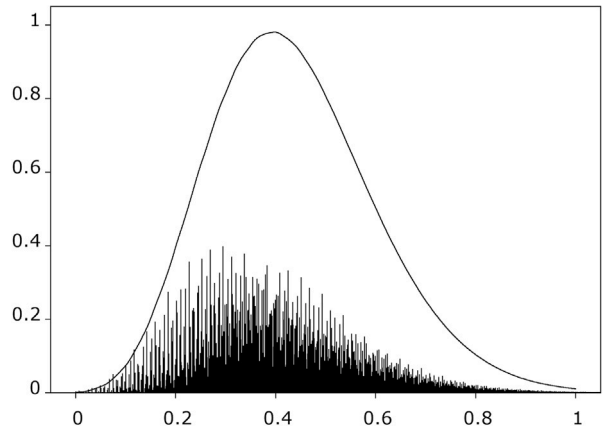

Fig. 3. Vibrational progression for the transition from the vibronic ground state of $UO_2Cl_2^-$ to vibrational states of the ground electronic state of UO_2Cl_2 obtained from Franck–Condon (FC) simulation using the harmonic approximation. The x axis denotes vibrational energies (in eV) with the origin set as the value of the origin transition. simulation convoluted to the experimental resolution The broad curve is obtained by convoluting the stick spectrum with a half width at half maximum value of 0.1 eV. A value of 0.397 eV for the difference between EA_a and ADE was obtained as the shift between the threshold and the maximum peak position in this FC progression.

4. Results and discussion

The geometry optimization at the SFX2C-1e-CCSD(T)/cc-pVTZ level produced a C_{2v} equilibrium structure for the ground state of UO_2Cl_2. The computed structural parameters for UO_2Cl_2 as summarized in Table 1 are consistent with previous computational results [37,49]. Fig. 2 shows the four lowest electronic states of $UO_2Cl_2^-$ and the molecular orbitals in which the unpaired electron is located. The extra electron of the $UO_2Cl_2^-$ anion largely occupies a U 5f orbital. The presence of the additional U 5f electron introduces significant repulsion with the U–O and U–Cl bonds. Consequently, as shown in Table 1, the U–O and U–Cl bond lengths in the anionic states are considerably longer than those in the neutral molecule. In particular, the U–Cl bond length is elongated by more than 0.15 Å. The O–U–O angle is also considerably reduced. The increase of the bond lengths is expected to weaken the U–O and U–Cl bonds. Indeed, vibrational frequencies of the $UO_2Cl_2^-$ anion are consistently lower than those in the neutral molecule. As shown in Table 2, the harmonic vibrational frequencies are reduced by around 10% for the symmetric U–O stretching mode and more than 20% for the symmetric U–Cl stretching mode. Even the harmonic vibrational frequency for the symmetric O–U–O bending mode is decreased by around 15%.

Spin–orbit coupling tends to stabilize the 5f electron and increase the adiabatic electron affinity (EA_a). As shown in Table 3, the SO correction to the EA_a amounts to around 0.31 eV. We mention that the basis-set error for cc-pVTZ-unc basis sets is around 0.25 eV. The computed EA_a at the SFX2C-1e-CCSD(T) level amounts to 2.582 eV for cc-pVTZ-unc basis sets, 2.727 eV for cc-pVQZ-unc basis sets, and 2.820 eV when extrapolated to estimate the basis-set-limit value. It is clearly important to take both SO correction and basis-set effects into account when conducting accurate calculations of the EA_a value of UO_2Cl_2. The zero-point vibrational (ZPV) correction plays a relatively minor role. The ZPV contribution reduces EA_a by 0.028 eV, since the vibrational frequencies of the anion are lower than those of the neutral molecule. Altogether, these give a value of 3.153 eV for EA_a of UO_2Cl_2. The vertical detachment energy (VDE) of $UO_2Cl_2^-$ was then obtained by adding the difference between the maximal peak position and the origin, both in the calculated FC spectrum, to the computed EA_a value. This difference, derived from Fig. 3, has a value of 0.397 eV. The resulting computed VDE is thus 3.550 eV.

Figs. 4a and 4b present the PES of $UO_2Cl_2^-$ taken with a 355 nm (3.49 eV) and a 266 nm (4.66 eV) laser, respectively. The appreciable width of peak "X" ranging from 3 to 4 eV in Fig. 4b signifies a significant difference between the equilibrium structures of UO_2Cl_2 and $UO_2Cl_2^-$. The progression observed in the photoelectron spectrum (Fig. 4b) is also consistent with the vibrational progression obtained from calculations (Fig. 3). The VDE value is the vertical photodetachment transition energy from the vibronic ground state of the anion to the electronic ground state of the neutral molecule at the geometry of its anion. This transition energy corresponds to the point of the greatest Franck–Condon vibrational overlap and is revealed in the PE spectrum by the EBE of its intensity maximum. Thus, the experimentally-determined VDE value is 3.69 eV, the EBE of the intensity maximum of the most intense peak X in the anion photoelectron spectrum shown in Fig. 4b. We assess an uncertainty of ±0.20 eV. Because they are due to maximal FC overlap, experimental VDE values can be definitively determined by inspection, i.e., by locating the EBE of the

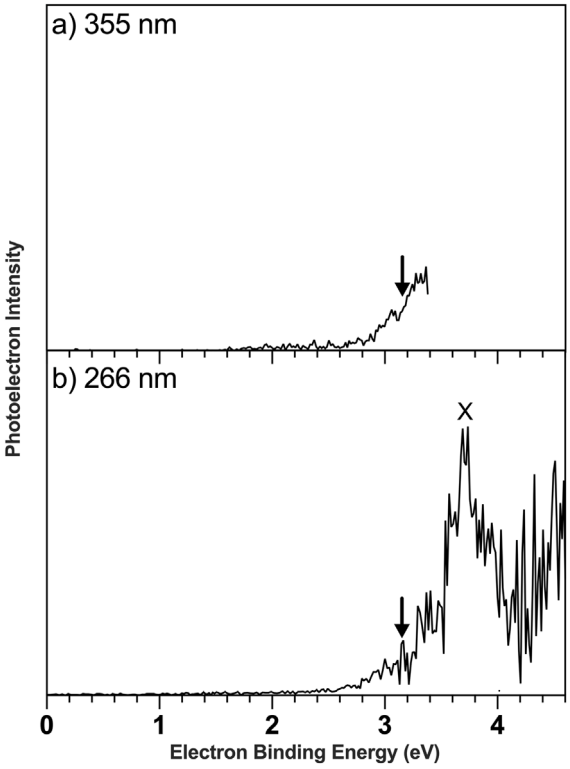

Fig. 4. The photoelectron spectra of $UO_2Cl_2^-$ obtained using (a) the third harmonic (355 nm, 3.49 eV) and (b) the fourth harmonic of an Nd:YAG laser (266 nm, 4.66 eV). The arrows designate the position of the computed value of 3.15 eV for the adiabatic electron affinity.

intensity maximum in the ground state anion to ground state neutral photoelectron spectral band. This resulting experimentally-determined VDE value of 3.69±0.20 eV is in good agreement with the computed value of 3.550 eV. Regarding the computed VDE value based on the FC simulation shown in Fig. 3, the anharmonic contribution tends to redistribute intensities to the transitions at vibrational states with higher vibrational quantum numbers. Thus, the present FC simulation shown in Fig. 3, which uses the harmonic approximation, leads to a slight underestimation of the actual VDE value. This is consistent with the computed value versus measured VDE values reported here.

The electron binding energy of the origin transition in an anion photoelectron spectrum is equal to the EA_a value of the anion's neutral counterpart. However, while the VDE value can be located by inspection of the PE spectrum, the origin transition must be assigned, and this can be challenging due to several factors. First, due to significant structural relaxation, the origin transition of the $UO_2Cl_2^-$ photoelectron spectrum exhibits inherently weak intensity, as clearly demonstrated in the FC simulation in Fig. 3. Add low pre-photodetachment $UO_2Cl_2^-$ anion intensity to the picture, and a modest signal-to-noise spectrum is the result. Next, consider the possibility of vibrational hot bands. In an ideal anion PE spectrum the EBE of the intensity threshold would reveal the origin. However, if some anion vibrational levels above v = 0 were to be populated, the EBE of the threshold would be slightly less than the EBE of the true origin. Laser vaporization anion sources are characterized by a competition between high temperatures due to the plasma produced in a laser strike and adiabatic cooling due to the rapid expansion of helium carrier gas. While the resulting temperature of the anions and thus the prevalence of hot bands varies considerably, some extent of hot band presence is common, making the threshold determination of the origin uncertain. While nascent anion temperatures of a few hundred degrees are often extracted from FC fits when the anions have simple structures, these are of minimal value given that the anions are not in equilibrium and thus do not conform to the Boltzmann distribution.

The central issue in the present study is the experimental-determination of the EA_a value of UO_2Cl_2. The origin transition is almost certainly one of the weakly discernible peaks in the PE spectrum between the hot-band-dominated threshold region and peak, X, from which the VDE value was assigned by inspection. Given the definitions of EA_a and VDE, the EA_a-determining origin transition typically sits at a lower EBE than the VDE transition by a few tenths of an eV. Given the foregoing, we assign the EA_a value of UO_2Cl_2 to be 3.2 ± 0.20 eV based of the PE spectrum of $UO_2Cl_2^-$. This same region of the spectrum is shown in Fig. 4a, which was measured using 355 nm photons and thus does not cover the VDE region of the spectrum. It too is consistent with this assignment. The present high-level calculations found the EA_a value of UO_2Cl_2 to be 3.15 eV and the VDE value of $UO_2Cl_2^-$ to be 3.55 eV. Experimental measurements based on the PE spectrum of $UO_2Cl_2^-$ determined EA_a value to be 3.2 ± 0.20 eV and the VDE value to be 3.69 ± 0.20 eV, both in good agreement with the computed value. All considered, we assert that our theoretically-determined and experimentally-supported value of 3.15 eV is a reliable assessment of the EA_a of UO_2Cl_2.

5. Conclusion and outlook

A joint computational–experimental study of the photoelectron spectrum of the uranyl dichloride anion, $UO_2Cl_2^-$, is reported. High-level relativistic coupled-cluster calculations predict that the photodetachment of $UO_2Cl_2^-$ involves a U 5f electron and induces significant geometry change. The electron affinity of uranyl dichloride neutral molecule, UO_2Cl_2, thus provides information about the U 5f orbital energy in UO_2Cl_2. In the future it would be interesting to determine electron affinities for other uranyl-containing molecules using photoelectron spectroscopy and relativistic coupled-cluster calculations, to obtain insights about the effects of ligands on the uranium 5f orbital energies of the uranyl ion.

CRediT authorship contribution statement

Mary Marshall: Collected the experiment data, Analyzed the experimental spectrum, Writing of the manuscript. **Zhaoguo Zhu:** Collected the experiment data, Analyzed the experimental spectrum, Writing of the manuscript. **Junzi Liu:** Performed calculations and analyzed the computational results, Writing of the manuscript. **Kit H. Bowen:** Conceptualization, Analyzed the experimental spectrum, Writing of the manuscript. **Lan Cheng:** Conceptualization, Performed calculations and analyzed the computational results, Writing of the manuscript.

Declaration of competing interest

The authors declare that they have no known competing financial interests or personal relationships that could have appeared to influence the work reported in this paper.

Acknowledgments

All computations in this work were carried out using Maryland Advanced Research Computing Center (MARCC). L. C. is indebted to John Stanton (Gainesville) for helpful discussions about Franck–Condon simulation with the harmonic approximation. The computational work has been supported by the Department of Energy, Office of Science, Office of Basic Energy Sciences, USA under Award Number DE-SC0020317 (L. C.). The experimental portion of this material is based upon work supported by the U.S. Department of Energy (DOE), Office of Science, Office of Basic Energy Sciences, Heavy Element Chemistry, USA program under Award Number, DE-SC0019317 (K.H.B).

References

[1] R.G. Denning, Electronic Structure and Bonding in Actinyl Ions BT - Complexes, Clusters and Crystal Chemistry, Springer Berlin Heidelberg, Berlin, Heidelberg, 1992, pp. 215–276.

[2] R.G. Denning, Electronic structure and bonding in actinyl ions and their analogs, J. Phys. Chem. A 111 (2007) 4125–4143.

[3] P.L. Arnold, J.B. Love, D. Patel, Pentavalent uranyl complexes, Coord. Chem. Rev. 253 (2009) 1973–1978.

[4] B.E. Cowie, J.M. Purkis, J. Austin, J.B. Love, P.L. Arnold, Thermal and photochemical reduction and functionalization chemistry of the uranyl dication, $[U^{VI}O_2]^{2+}$, Chem. Rev. 119 (2019) 10595–10637.

[5] J. Veliscek-Carolan, Separation of actinides from spent nuclear fuel: A review, J. Hazard. Mater. 318 (2016) 266–281.

[6] F.V. Stohl, D.K. Smith, The crystal chemistry of the uranyl silicate minerals, Am. Mineral. 66 (1981) 610–625.

[7] C.K. Jørgensen, R. Reisfeld, Uranyl Photophysics BT - Topics in Inorganic and Physical Chemistry, Springer Berlin Heidelberg, Berlin, Heidelberg, 1982, pp. 121–171.

[8] C. Görller-Walrand, S. De Houwer, L. Fluyt, K. Binnemans, Spectroscopic properties of uranyl chloride complexes in non-aqueous solvents, Phys. Chem. Chem. Phys. 6 (2004) 3292–3298.

[9] R.D. Hunt, L. Andrews, Reactions of pulsed?laser evaporated uranium atoms with molecular oxygen: Infrared spectra of UO, UO_2, UO_3, UO_2^+, UO_2^{2+}, and UO_3-o_2 in solid argon, J. Chem. Phys. 98 (1993) 3690–3696.

[10] J.C. Krupa, E. Simoni, J. Sytsma, N. Edelstein, Optical spectroscopic studies of uranyl chloride UO_2cl_2, J. Alloys Compd. 213–214 (1994) 471–474.

[11] H.H. Cornehl, C. Heinemann, J. Marçalo, A.P. de Matos, H. Schwarz, The bare uranyl(2+) ion, UO_2^{2+}, Angew. Chem., Int. Ed. Engl. 35 (1996) 891–894.

[12] M.J. Sarsfield, M. Helliwell, Extending the chemistry of the uranyl ion: Lewis acid coordination to a UO oxygen, J. Am. Chem. Soc. 126 (2004) 1036–1037.

[13] S.P. Pasilis, J.E. Pemberton, Speciation and coordination chemistry of uranyl(VI)-citrate complexes in aqueous solution, Inorg. Chem. 42 (2003) 6793–6800.

[14] P.L. Arnold, D. Patel, C. Wilson, J.B. Love, Reduction and selective oxo group silylation of the uranyl dication, Nature 451 (2008) 315–317.

[15] J. Jin, R. Gondalia, M.C. Heaven, Electronic spectroscopy of UO_2cl_2 isolated in solid Ar, J. Phys. Chem. A 113 (2009) 12724–12728.

[16] P.L. Arnold, A.F. Pécharman, E. Hollis, A. Yahia, L. Maron, S. Parsons, J.B. Love, Uranyl oxo activation and functionalization by metal cation coordination, Nature Chem. 2 (2010) 1056–1061.

[17] P.L. Arnold, E. Hollis, F.J. White, N. Magnani, R. Caciuffo, J.B. Love, Single-electron uranyl reduction by a rare-earth cation, Angew. Chem., Int. Ed. Engl. 50 (2011) 887–890.

[18] P.L. Arnold, G.M. Jones, S.O. Odoh, G. Schreckenbach, N. Magnani, J.B. Love, Strongly coupled binuclear uranium-oxo complexes from uranyl oxo rearrangement and reductive silylation, Nature Chem. 4 (2012) 221–227.

[19] R.J. Baker, New reactivity of the uranyl(VI) ion, Chem. Eur. J. 18 (2012) 16258–16271.

[20] P.D. Dau, J. Su, H.T. Liu, D.L. Huang, J. Li, L.S. Wang, Photoelectron spectroscopy and the electronic structure of the uranyl tetrachloride dianion: $UO_2Cl_4^{2-}$, J. Chem. Phys. 137 (2012) 064315.

[21] J. Su, P.D. Dau, Y.H. Qiu, H.T. Liu, C.F. Xu, D.L. Huang, L.S. Wang, J. Li, Inorg. Chem. 52 (2013) 6617–6626.

[22] M.J. Van Stipdonk, M. d. C. Michelini, A. Plaviak, D. Martin, J.K. Gibson, Formation of bare UO_2^{2+} and NUO^+ by fragmentation of gas-phase uranyl?acetonitrile complexes, J. Phys. Chem. A 118 (2014) 7838–7846.

[23] J. Su, W.-L. Li, G.V. Lopez, T. Jian, G.-J. Cao, W.-L. Li, W.H.E. Schwarz, L.-S. Wang, J. Li, Probing the electronic structure and chemical bonding of mono-uranium oxides with different oxidation states: UO_x and UO_x^- (x = 3 – 5), J. Phys. Chem. A 120 (2016) 1084–1096.

[24] M.C. Kirkegaard, J. Langford, J. Steill, B. Anderson, A. Miskowiec, Vibrational properties of anhydrous and partially hydrated uranyl fluoride, J. Chem. Phys. 146 (2017) 024502.

[25] P.J. Skrodzki, M. Burger, L.A. Finney, F. Poineau, S.M. Balasekaran, J. Nees, K.R. Czerwinski, I. Jovanovic, Ultrafast laser filament-induced fluorescence spectroscopy of uranyl fluoride, Sci. Rep. 8 (2018) 11629.

[26] J.H. Marks, P. Kahn, M. Vasiliu, D.A. Dixon, M.A. Duncan, Photodissociation and theory to investigate uranium oxide cluster cations, J. Phys. Chem. A 124 (2020) 1940–1953.

[27] A.R. Bubas, E. Perez, L.J. Metzler, S.D. Rissler, M.J. Van Stipdonk, Collision-induced dissociation of $[UO_2(NO_3)_3]^-$ and $[UO_2(NO_3)_2(O_2)]^-$ and reactions of product ions with H_2O and O_2, J. Mass Spectrom. n/a (2021) e4705.

[28] P. Pyykkö, L.J. Laakkonen, K. Tatsumi, REX calculations. 12. iteration parameters for the 5f-element organometallics of thorium-neptunium. Geometries of ThO_2 and UO_2^{2+} revisited, Inorg. Chem. 28 (1989) 1801–1805.

[29] M. Pepper, B.E. Bursten, The electronic structure of actinide-containing molecules: A challenge to applied quantum chemistry, Chem. Rev. 91 (1991) 719–741.

[30] W.A. de Jong, L. Visscher, W.C. Nieuwpoort, On the bonding and the electric field gradient of the uranyl ion, J. Mol. Struct. THEOCHEM 458 (1998) 41–52.

[31] S. Spencer, L. Gagliardi, N.C. Handy, A.G. Ioannou, C.-K. Skylaris, A. Willetts, A.M. Simper, Hydration of UO_2^{2+} and PuO_2^{2+}, J. Phys. Chem. A 103 (1999) 1831–1837.

[32] Z. Zhang, R.M. Pitzer, Application of relativistic quantum chemistry to the electronic energy levels of the uranyl ion, J. Phys. Chem. A 103 (1999) 6880–6886.

[33] Q. Wang, R.M. Pitzer, Structure and spectra of UO_2F_2 and its hydrated species, J. Phys. Chem. A 105 (2001) 8370–8375.

[34] S. Matsika, R.M. Pitzer, Actinyl ions in $Cs_2UO_2Cl_4$, J. Phys. Chem. A 105 (2001) 637–645.

[35] S. Matsika, Z. Zhang, S.R. Brozell, J.-P. Blaudeau, Q. Wang, R.M. Pitzer, Electronic structure and spectra of actinyl ions, J. Phys. Chem. A 105 (2001) 3825–3828.

[36] D. Majumdar, K. Balasubramanian, H. Nitsche, A comparative theoretical study of bonding in UO_2^{++}, UO_2^+, UO_2, UO_2^-, OUCO, $O_2U(CO)_2$ and UO_2CO_3, Chem. Phys. Lett. 361 (2002) 143–151.

[37] A. Kovács, R.J.M. Konings, Theoretical study of UX_6 and UO_{22} (X = F, Cl, Br, I), J. Mol. Struct. THEOCHEM 684 (2004) 35–42.

[38] W.A. de Jong, E. Aprà, T.L. Windus, J.A. Nichols, R.J. Harrison, K.E. Gutowski, D.A. Dixon, Complexation of the carbonate, nitrate, and acetate anions with the uranyl dication: Density functional studies with relativistic effective core potentials, J. Phys. Chem. A 109 (2005) 11568–11577.

[39] K. Pierloot, E. van Besien, Electronic structure and spectrum of UO_2^{2+} and $UO_2Cl_4^{2-}$, J. Chem. Phys. 123 (2005) 204309.

[40] D. Hagberg, G. Karlström, B.O. Roos, L. Gagliardi, The coordination of uranyl in water: A combined quantum chemical and molecular simulation study, J. Am. Chem. Soc. 127 (2005) 14250–14256.

[41] J.L. Sonnenberg, P.J. Hay, R.L. Martin, B.E. Bursten, Theoretical investigations of uranyl-ligand bonding: Four- and five-coordinate uranyl cyanide, isocyanide, carbonyl, and hydroxide complexes, Inorg. Chem. 44 (2005) 2255–2262.

[42] E. van Besien, K. Pierloot, C. Görller-Walrand, Electronic spectra of uranyl chloride complexes in acetone: a CASSCF/CASPT2 investigation, Phys. Chem. Chem. Phys. 8 (2006) 4311–4319.

[43] M. García-Hernández, C. Willnauer, S. Krüger, L.V. Moskaleva, N. Rösch, Systematic DFT study of gas phase and solvated uranyl and neptunyl complexes $[AnO_2X_4]^n$ (An = U, Np; X = F, Cl, OH, n = −2; X = H_2O, n = +2), Inorg. Chem. 45 (2006) 1356–1366.

[44] K. Pierloot, E. van Besien, E. van Lenthe, E.J. Baerends, Electronic spectrum of UO_2^{2+} and $[UO_2Cl_4]^{2-}$ calculated with time-dependent density functional theory, J. Chem. Phys. 126 (2007) 194311.

[45] I. Infante, E. Eliav, M.J. Vilkas, Y. Ishikawa, U. Kaldor, L. Visscher, A Fock space coupled cluster study on the electronic structure of the UO_2, UO_2^+, U^{4+}, and U^{5+} species, J. Chem. Phys. 127 (2007) 124308.

[46] G.A. Shamov, G. Schreckenbach, T.N. Vo, A comparative relativistic DFT and Ab initio study on the structure and thermodynamics of the oxofluorides of uranium(IV), (V) and (VI), Chem. Eur. J. 13 (2007) 4932–4947.

[47] F. Real, A.S.P. Gomes, L. Visscher, V. Vallete, E. Eliav, Benchmarking electronic structure calculations on the bare UO_2^{2+} ion: How different are single and multireference electron correlation methods? J. Phys. Chem. A 113 (2009) 12504–12511.

[48] B. Vlaisavljevich, L. Gagliardi, P.C. Burns, Understanding the structure and formation of uranyl peroxide nanoclusters by quantum chemical calculations, J. Am. Chem. Soc. 132 (2010) 14503–14508.

[49] J. Su, Y.-L. Wang, F. Wei, W.H.E. Schwarz, J. Li, Theoretical study of the luminescent states and electronic spectra of UO_2Cl_2 in an argon matrix, J. Chem. Theory Comput. 7 (2011) 3293–3303.

[50] F. Wei, G. Wu, W.H.E. Schwarz, J. Li, Geometries, electronic structures, and excited states of UN_2, NUO^+, and UO_2^{2+}: a combined CCSD(T), RAS/CASPT2 and TDDFT study, Theor. Chem. Acc. 129 (2011) 467–481.

[51] P. Tecmer, A.S.P. Gomes, U. Ekström, L. Visscher, Electronic spectroscopy of UO_2^{2+}, NUO^+ and NUN: an evaluation of time-dependent density functional theory for actinides, Phys. Chem. Chem. Phys. 13 (2011) 6249–6259.

[52] P. Tecmer, A. Severo Pereira Gomes, S. Knecht, L. Visscher, Communication: Relativistic fock-space coupled cluster study of small building blocks of larger uranium complexes, J. Chem. Phys. 141 (2014) 41107.

[53] A. Kovács, R.J.M. Konings, J.K. Gibson, I. Infante, L. Gagliardi, Quantum chemical calculations and experimental investigations of molecular actinide oxides, Chem. Rev. 115 (2015) 1725–1759.

[54] J.K. Gibson, H.-S. Hu, M.J. Van Stipdonk, G. Berden, J. Oomens, J. Li, Infrared multiphoton dissociation spectroscopy of a gas-phase complex of uranyl and 3-oxa-glutaramide: An extreme red-shift of the $[o=u=o]^{2+}$ asymmetric stretch, J. Phys. Chem. A 119 (2015) 3366–3374.

[55] A.H. Greif, P. Hrobárik, J. Autschbach, M. Kaupp, Giant spin?orbit effects on 1H and 13C NMR shifts for uranium(vi) complexes revisited: role of the exchange?correlation response kernel, bonding analyses, and new predictions, Phys. Chem. Chem. Phys. 18 (2016) 30462–30474.

[56] S. Zhang, F. Wang, Excitation energies of UO_2^{2+}, NUO^+, and NUN based on equation-of-motion coupled-cluster theory with spin?orbit coupling, J. Phys. Chem. A 121 (2017) 3966–3975.

[57] L. Cheng, A study of non-iterative triples contributions in relativistic equation-of-motion coupled-cluster calculations using an exact two-component hamiltonian with atomic mean-field spin–orbit integrals: Application to uranyl and other heavy-element compounds, J. Chem. Phys. 151 (2019) 104103.

[58] M. Vasiliu, T. Jian, J.K. Gibson, K.A. Peterson, D.A. Dixon, A computational assessment of actinide dioxide cations AnO_2^{2+} for An = U to Lr: The limited stability range of the hexavalent actinyl moiety, $[O=An=O]^{2+}$, Inorg. Chem. 59 (2020) 4554–4566.

[59] R. Feng, E.D. Glendening, K.A. Peterson, Coupled cluster study of the interactions of AnO_2, AnO_2^+, and AnO_2^{2+} (An = U, Np) with N_2 and CO, Inorg. Chem. 59 (2020) 4753–4763.

[60] O. Ordoñez, X. Yu, G. Wu, J. Autschbach, T.W. Hayton, Synthesis and characterization of two uranyl-aryl ?Ate? Complexes, Chem. Eur. J. n/a (2020) http://dx.doi.org/10.1002/chem.202005078.

[61] W.L. Li, J. Su, T. Jian, G.V. Lopez, H.S. Hu, G.J. Cao, J. Li, L.S. Wang, Strong electron correlation in UO_2^-: A photoelectron spectroscopy and relativistic quantum chemistry study, J. Chem. Phys. 140 (2014) 094306.

[62] J. Czekner, G.V. Lopez, L.-S. Wang, High resolution photoelectron imaging of UO^- and UO_2^- and the low-lying electronic states and vibrational frequencies of UO and UO_2, J. Chem. Phys. 141 (2014) 244302.

[63] M. Gerhards, O.C. Thomas, J.M. Nilles, W.-J. Zheng, K.H. Bowen, Cobalt?benzene cluster anions: Mass spectrometry and negative ion photoelectron spectroscopy, J. Chem. Phys. 116 (2002) 10247–10252.

[64] J. Ho, K.M. Ervin, W.C. Lineberger, Photoelectron spectroscopy of metal cluster anions: Cu_n^-, Ag_n^-, and Au_n^-, J. Chem. Phys. 93 (1990) 6987–7002.

[65] J.F. Stanton, J. Gauss, L. Cheng, M.E. Harding, D.A. Matthews, P.G. Szalay, CFOUR, Coupled-Cluster techniques for Computational Chemistry, a quantum-chemical program package, With contributions from A.A. Auer, R.J. Bartlett, U. Benedikt, C. Berger, D.E. Bernholdt, S. Blaschke, Y. J. Bomble, S. Burger, O. Christiansen, D. Datta, F. Engel, R. Faber, J. Greiner, M. Heckert, O. Heun, M. Hilgenberg, C. Huber, T.-C. Jagau, D. Jonsson, J. Jusélius, T. Kirsch, K. Klein, G.M. KopperW.J. Lauderdale, F. Lipparini, T. Metzroth, L.A. Mück, D.P. O'Neill, T. Nottoli, D.R. Price, E. Prochnow, C. Puzzarini, K. Ruud, F. Schiffmann, W. Schwalbach, C. Simmons, S. Stopkowicz, A. Tajti, J. Vázquez, F. Wang, J.D. Watts and the integral packages MOLECULE (J. Almlöf and P.R. Taylor), PROPS (P.R. Taylor), ABACUS (T. Helgaker, H.J. Aa. Jensen, P. Jørgensen, and J. Olsen), and ECP routines by A. V. Mitin and C. van Wüllen. For the current version, see http://www.cfour.de.

[66] D.A. Matthews, L. Cheng, M.E. Harding, F. Lipparini, S. Stopkowicz, T.-C. Jagau, P.G. Szalay, J. Gauss, J.F. Stanton, Coupled-cluster techniques for computational chemistry: The CFOUR program package, J. Chem. Phys. 152 (2020) 214108.

[67] J.D. Watts, J. Gauss, R.J. Bartlett, Open-shell analytical energy gradients for triple excitation many-body, coupled-cluster methods: MBPT(4), CCSD+T(CCSD), CCSD(T), and QCISD(T), J. Chem. Phys. 200 (1992) 1–7.

[68] J.F. Stanton, C.L. Lopreore, J. Gauss, The equilibrium structure and fundamental vibrational frequencies of dioxirane, J. Chem. Phys. 108 (1998) 7190–7196.

[69] L. Cheng, J. Gauss, Analytic energy gradients for the spin-free exact two-component theory using an exact block diagonalization for the one-electron Dirac Hamiltonian, J. Chem. Phys. 135 (2011) 084114.

[70] S.M. Rabidoux, V. Eijkhout, J.F. Stanton, A highly-efficient implementation of the Doktorov recurrence equations for Franck–Condon calculations, J. Chem. Theory Comput. 12 (2016) 728–739.

[71] J. Liu, L. Cheng, An atomic mean-field spin–orbit approach within exact two-component theory for a non-perturbative treatment of spin–orbit coupling, J. Chem. Phys. 148 (2018) 144108.

[72] J. Liu, Y. Shen, A. Asthana, L. Cheng, Two-component relativistic coupled-cluster methods using mean-field spin–orbit integrals, J. Chem. Phys. 148 (2018) 034106.

[73] K. Raghavachari, G.W. Trucks, J.A. Pople, M. Head-Gordon, A fifth-order perturbation comparison of electron correlation theories, Chem. Phys. Lett. 157 (1989) 479–483.

[74] R.J. Bartlett, J.D. Watts, S.A. Kucharski, J. Noga, Non-iterative fifth-order triple and quadruple excitation energy corrections in correlated methods, Chem. Phys. Lett. 165 (1990) 513–522.

[75] K.A. Peterson, Correlation consistent basis sets for actinides. I. The Th and U atoms, J. Chem. Phys. 142 (2015) 74105.

[76] T.H. Dunning Jr., Gaussian basis sets for use in correlated molecular calculations. I. The atoms boron through neon and hydrogen, J. Chem. Phys. 90 (1989) 1007–1023.

[77] K.G. Dyall, Interfacing relativistic and nonrelativistic methods. IV. One- and two-electron scalar approximations, J. Chem. Phys. 115 (2001) 9136–9143.

[78] W. Liu, D. Peng, Exact two-component Hamiltonians revisited, J. Chem. Phys. 131 (2009) 1–5.

[79] M. Nooijen, R.J. Bartlett, Equation of motion coupled cluster method for electron attachment, J. Chem. Phys. 102 (1995) 3629–3647.

[80] T. Helgaker, W. Klopper, H. Koch, J. Noga, Basis-set convergence of correlated calculations on water, J. Chem. Phys. 106 (1997) 9639–9646.

[81] K.G. Dyall, Interfacing relativistic and nonrelativistic methods. I. Normalized elimination of the small component in the modified Dirac equation, J. Chem. Phys. 106 (1997) 9618–9626.

[82] W. Kutzelnigg, W. Liu, Quasirelativistic theory equivalent to fully relativistic theory, J. Chem. Phys. 123 (2005) 241102.

[83] M. Iliaš, T. Saue, An infinite-order two-component relativistic hamiltonian by a simple one-step transformation, J. Chem. Phys. 126 (2007) 64102.

[84] B.A. Heß, C.M. Marian, U. Wahlgren, O. Gropen, A mean-field spin–orbit method applicable to correlated wavefunctions, Chem. Phys. Lett. 251 (1996) 365–371.